

# Plasma enhanced synthesis of N doped vertically aligned carbon nanofibers on 3D graphene

Siddharth Mishra<sup>1</sup>  | Hung Nguyen<sup>2</sup> | Paa Kwasi Adusei<sup>1</sup> | Yu-Yun Hsieh<sup>1</sup> | Vesselin Shanov<sup>1,2</sup>

<sup>1</sup> Department of Materials Science and Engineering, University of Cincinnati, OH 45221, USA

<sup>2</sup> Department of Chemical and Environmental Engineering, University of Cincinnati, OH 45221, USA

#### Correspondence

Vesselin Shanov, Department of Materials Science and Engineering, University of Cincinnati, OH 45221, USA.

Email: shanovvn@ucmail.uc.edu

#### Funding information

NSF, Grant/Award Number: SBET 1706489

Graphene and carbon nanotubes/fibers (CNT/CNF) hybrid structures are emerging as frontier materials for high-efficiency electronics, energy storage, thermoelectric, and sensing applications owing to the utilization of extraordinary electrical and physical properties of both nanocarbon materials. Recent advances show a successful improvement in the structure and surface area of layered graphene by incorporating another dimension and structural form—three-dimensional graphene (3DG). In this study, vertically aligned CNFs were grown using plasma enhanced chemical vapor deposition on a relatively new form of compressed 3DG. The latter was synthesized using a conventional thermal chemical vapor deposition. The resulting free-standing hybrid material is *in-situ* N doped during synthesis by ammonia plasma and is produced in the form of a hybrid paper. Characterization of this material was done using electrochemical and spectroscopic measurements. The N doped hybrid showed relatively higher surface area and improved areal current density in electrochemical measurements than compressed pristine 3DG, which makes it a potential candidate for use as an electrode material for supercapacitors, sensors, and electrochemical batteries.

#### KEYWORDS

CNF, CNT, CVD, graphene, N doping, plasma

## 1 | INTRODUCTION

Plasma enhanced chemical vapor deposition (PECVD) has proved to be a crucial technique for synthesizing carbon-based materials like carbon nanofibers (CNFs),<sup>1</sup> carbon nanotubes (CNTs),<sup>2</sup> graphene,<sup>3</sup> carbon nanowalls,<sup>4</sup> and diamond.<sup>5</sup> High-mobility graphene on copper foil has been synthesized at temperatures below 420°C using PECVD.<sup>6</sup> This synthesis approach, besides having advantages like low-temperature growth and vertical alignment of nanostructures, also offers good quality and adhesion of carbon structures to the substrates.<sup>7</sup> Various substrates have been used for vertically aligned CNT (VACNTs) and CNFs growth like metals,<sup>8</sup> silicon,<sup>9</sup> and quartz.<sup>10</sup> Direct PECVD growth of vertically oriented graphene on Au interdigitated field-effect transistor biosensor has also been reported.<sup>11</sup> The hybrid growth of CNT-graphene is an area of greater interest as in that case, utilization of extraordinary electrical

and mechanical properties of both carbon nanomaterials becomes possible. As an attempt at synthesizing carbon nanomaterial hybrids, the growth of CNT on graphene and graphene on CNT, both have been reported. The growth of graphene on the tips of CNT has been done successfully in a one-step process by Choi et al.<sup>12</sup> Another study was reported by our group which involved the growth of mushroom gills-like graphene flakes on top of CNT arrays.<sup>13</sup> The other configuration, ie, CNT on graphene has been explored by Zhao et al.,<sup>14</sup> Kim et al.,<sup>15</sup> and others. Most of these studies focus on thermal CVD of CNTs on graphene. Apart from the CVD stacking method, CNT-graphene hybrid films made by blown bubble method have been reported by Wu et al.<sup>16</sup> The nature of bonding between graphene and CNT has been confirmed to be covalent by scanning transmission electron microscopic studies.<sup>17</sup> This has further led to an increasing interest in the high strength graphene and CNT hybrid structures.

Over the years, the structure of graphene has evolved, and attempts to increase the surface area of multilayer and single layer graphene have led to the synthesis of three-dimensional graphene 3D graphene (3DG). The 3DG form has good conductivity, lightweight, stable, and scalable structure. Multiple ways of making 3DG have been reported. Cao et al<sup>18</sup> reported the use of Ni foam to grow 3DG foam-like structure. Our group in the past used Ni powder to synthesize 3DG pellets and graphene paper<sup>19,20</sup> Another interesting way of making a 3DG structure was reported by Huczko et al<sup>21</sup> by combustion of magnesium/calcium oxalates. A bottom-up approach like self-assembly has also been employed for synthesis of 3DG.<sup>22</sup> The 3DG-CNT hybrid in the form of aerogel has also been reported for use in Li-Se batteries.<sup>23</sup> Some general drawbacks of above reported 3DG structures include low conductivity, less purity, unstable structure, and difficulties in scaling up. In this study, a different method of synthesizing 3DG is illustrated, which uses a combination of polymer and nickel powder in a solvent to form a catalyst slurry. The conductivity of this type of 3DG obtained is higher as compared with 3DG foam.<sup>24</sup> The conductivity of the as-grown 3DG can be altered by compression using a roller press or hydraulic press. This also makes the as-grown 3DG denser and in the form of a sheet which can be used as a base electrode or substrate for hybridization with other materials.

Here, in this study, the “as grown” 3DG was compressed by a roller press and made into a square sheet. The conductivity of 3DG increased many folds after compression. This compressed and highly conductive 3DG was chosen as the substrate for the growth of vertically aligned CNF (VACNF) using PECVD. Use of PECVD is a perfect means of in-situ N doping of carbon nanostructures during synthesis. There are numerous benefits of having N doped carbon nanostructures.<sup>25</sup> N doping of graphene has been reported to enhance capacitance,<sup>26</sup> sensing efficiency,<sup>27</sup> and chemical activity<sup>28</sup> in the carbon structure. Doping of graphene using ammonia plasma has even been reported to shift its valence band by 0.2 eV.<sup>29</sup> Plasma treatment has also been shown to have some beneficial effects on structure and morphology like an increase in the surface area of carbon nanostructures.<sup>30</sup> Usually, the CNTs synthesized using PECVD are thicker in diameter (60–200 nm) and are more commonly referred to as CNFs. These CNFs can be used for different electrochemical applications just like thermal grown CNTs. A review of growth, properties, and application of CNFs can be found here.<sup>31</sup> After examining the individual properties of VACNFs and 3DG, it can be envisioned that the PECVD growth of VACNF on 3DG is expected to result in an efficient hybrid carbon structure.

The surface morphology and the internal structural properties of the N doped VACNF-3DG hybrid material have been investigated using scanning electron microscopy and Raman spectroscopy respectively. The species in plasma were in situ monitored using optical emission spectroscopy (OES). The hydrophilicity of the pristine 3DG and hybrid structure was evaluated by contact angle measurements. Since ammonia plasma was used during VACNF growth, the resultant structure is doped with nitrogen which was proved by X-ray photoelectron spectroscopy (XPS). The electrochemical response of the material was also tested against pristine 3DG using cyclic voltammetry. This novel free-standing hybrid structure synthesized

using a combination of thermal and plasma CVD described in our study illustrates the benefit of both carbon nanomaterials, as well as N doping. The cyclic voltammetry data indicates that the N doped hybrid structure exhibited better areal current density than compressed pristine 3DG and could potentially be used as an electrode for electrochemical sensors, batteries, and supercapacitors.

## 2 | EXPERIMENTAL

### 2.1 | Materials and methods

The synthesis of a relatively new form of low-cost 3DG was accomplished using conventional thermal CVD using nickel powder and polymer binder slurry cast into a sheet as catalyst and methane as the carbon source. This has been described in detail in our previous publication.<sup>32</sup> The resulting 3DG is lightweight (0.78 mg/cm<sup>2</sup>) and has a porous sheet-like structure. The “as grown” 3DG was ca. 163 μm thick after catalyst removal. The compression of 3DG was done to improve electrical properties and to get uniform growth of CNFs. The catalyst-free 3DG was dried in a vacuum oven, sandwiched between two 0.125 mm stainless steel foils, and compressed using a roller press with an adjustable gap. This adjustable gap distance leads to different thicknesses of 3DG which corresponded to different electrical conductivities. Table S1 in the supplementary information show the variation of 3DG conductivity with thickness and adjustable gap distance of the roller press. To get a thickness of about 5.5 μm, the gap distance used was 0.25 mm. This led to 96.6% reduction in 3DG volume and an increase in conductivity of 3DG from 20 to 760 S/cm. To make the N doped hybrid structure, the paper-like 3DG was transferred on a Si wafer using isopropanol for good adhesion and to prevent the possibility of being sucked by the vacuum pump during low-pressure PECVD. A thin film of Ni (7 nm) was deposited on 3DG/Si by e-beam evaporation. The growth of VACNFs on 3DG/Si was done using AIXTRON Black Magic PECVD system. The growth was carried out using acetylene (40 sccm) as a carbon source and ammonia (200 sccm) as the reducing gas for 10 minutes. A plasma power of 100 W was employed for the growth which was done at a relatively low temperature of 600°C. The species in the plasma were monitored using OES. The sample was collected after cooling the reactor to 150°C and venting out the gases. The product N doped VACNF-3DG hybrid material on the silicon wafer was peeled off carefully into a free-standing structure for further characterization and analysis. The detailed process schematic is shown in Figure 1. The resulting structure is a hybrid sheet/paper with one side as N doped VACNF and other as 3DG.

Scanning electron microscopy images were taken using FEI SCIOS SEM. A Philips CM-20 was used for transmission electron microscopic imaging. The samples were prepared by sonication of dispersion on Cu grids with lacey carbon film. A Renishaw spectrometer with 514-nm He-Ne laser, exposure time of 10 seconds, and spot size of 1 μm<sup>2</sup> was used for RAMAN characterization. During the PECVD deposition of VACNFs on 3DG, Ocean Optics HR 4000CG-UV-NIR with slit size of 10 μm was used to monitor in situ the species in ammonia and acetylene plasma. To improve the quality

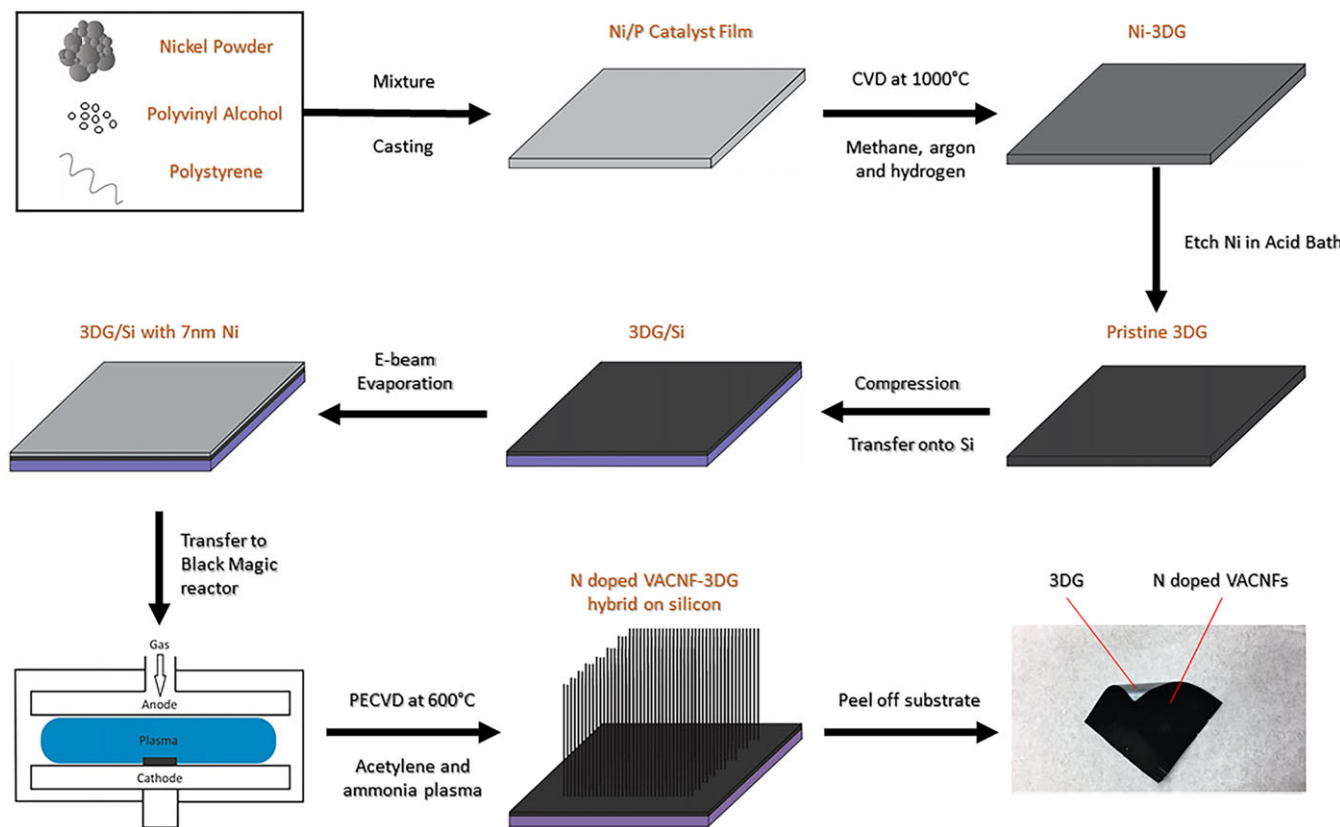


**FIGURE 1** Schematic of the fabrication process for making N-doped VACNF-3DG hybrid material

of the spectrum, a UV-VIS collimating lens was added to the fiber optic cable. The water contact angle on the VACNF-3DG surface was evaluated by a Model 590 Rame-hart Goniometer. For XPS, a VG Thermo-Scientific ML 3000 UHV surface analysis system was employed. The elemental peak deconvolution was done using Shirley-type baseline and pure Gaussian landscape. The hybrid sample was treated with 3 M HCl before XPS measurements to remove the Ni catalyst at the tips of VACNFs. The electrochemical studies were conducted using GAMRY potentiostat and 1 M  $\text{Na}_2\text{SO}_4$  as the electrolyte. The conductivity of 3DG and N-doped hybrid was measured using 873 Interface Module non-contact sheet resistance meter by Delcom instruments.

### 3 | RESULT AND DISCUSSION

To understand the composition of direct current gas plasma during the deposition of VACNFs on 3DG, OES was used as shown in Figure 2. The gases in the reactor mainly consisted of acetylene (40 sccm) and ammonia (200 sccm). Because of the higher flow rate, the OES spectrum was hugely dominated by ammonia OES peaks which included the three lines from Balmer series of the hydrogen spectrum— $\text{H}_\alpha$  (656.3 nm),  $\text{H}_\beta$  (486 nm), and  $\text{H}_\gamma$  (434 nm) lines. A peak belonging to N-H was seen around 336 nm in the spectrum. The electronic transition assigned to this peak is  $[\text{A}^3\pi - \text{X}^3\Sigma^-]$ . A couple of peaks belonging to second positive band  $\text{N}_2^+$  were seen around 391.1 (0,0), 317.0 (1,0), and 357.6 (0,1) nm with vibrational transition given in brackets. The electronic transition corresponding to this system is  $[\text{C}^3\Pi_u - \text{B}^3\Pi_g]$ <sup>33</sup>.

Two peaks contributing to carbon from acetylene were also noted around 468 and 589.9 nm, which can be referred to as  $\text{C}_2$  peaks.<sup>34</sup> These peaks represent species which are the building blocks of CNTs and CNFs. Another peak belonging to CH species can be seen around 387 nm before the second positive  $\text{N}_2$  band. Acetylene also could have contributed to the three H peaks. From the OES spectrum, it can be asserted that N-doping of the hybrid structure was facilitated by the generated N-based species yielded by the ammonia gas during the PECVD process.

The SEM image (Figure 3B) of compressed 3DG indicates planar surface morphology as compared with uncompressed 3DG (Figure S2). The VACNFs were approx. 10  $\mu\text{m}$  tall. The attachment of VACNFs to 3DG is shown in the cross-section image (Figure 3C). For comparison, SEM image of VACNFs deposited on uncompressed 3DG has been shown in Figure S3. Clearly, the number of VACNFs on compressed 3DG seemed to be higher as compared with uncompressed 3DG. This is one of the motivations behind using compressed 3DG, the other one being improved electrical conductivity. Usually, an oxide buffer layer is used to prevent diffusion of metal catalyst into the Si at high temperatures and plasma conditions, but in this case, we use 3DG as the base substrate, so we did not use any buffer layer making it a pure carbon hybrid structure. The TEM image (Figure 4) shows the VACNFs and 3DG next to each other. It may be connected but it is speculative, and more efforts are needed to zoom in the interface between the 3DG fragment and the VACNFs, which will require atomic resolution TEM imaging. The diameter of the individual CNFs as seen from Figure 4B is ca. 60 nm. The CNFs exhibit a typical

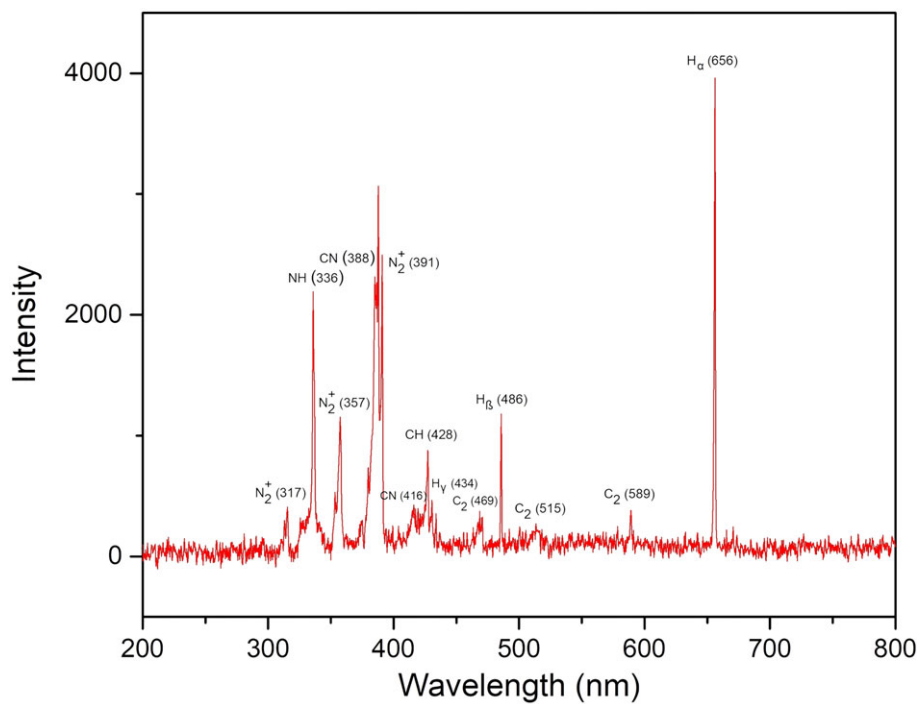


**FIGURE 2** Optical emission spectra for ammonia-acetylene plasma

bamboo-like structure with Ni catalyst particles encapsulated on their tips. Figure 5 reveals the RAMAN spectra for pristine 3DG and hybrid material. The spectrum for pristine 3DG was taken prior

to catalyst deposition which showed a very low-intensity D peak with G/D ratio to be 14.2, which indicated low defect and high purity of 3DG.<sup>35</sup> The first-order scattering graphitic peak G around

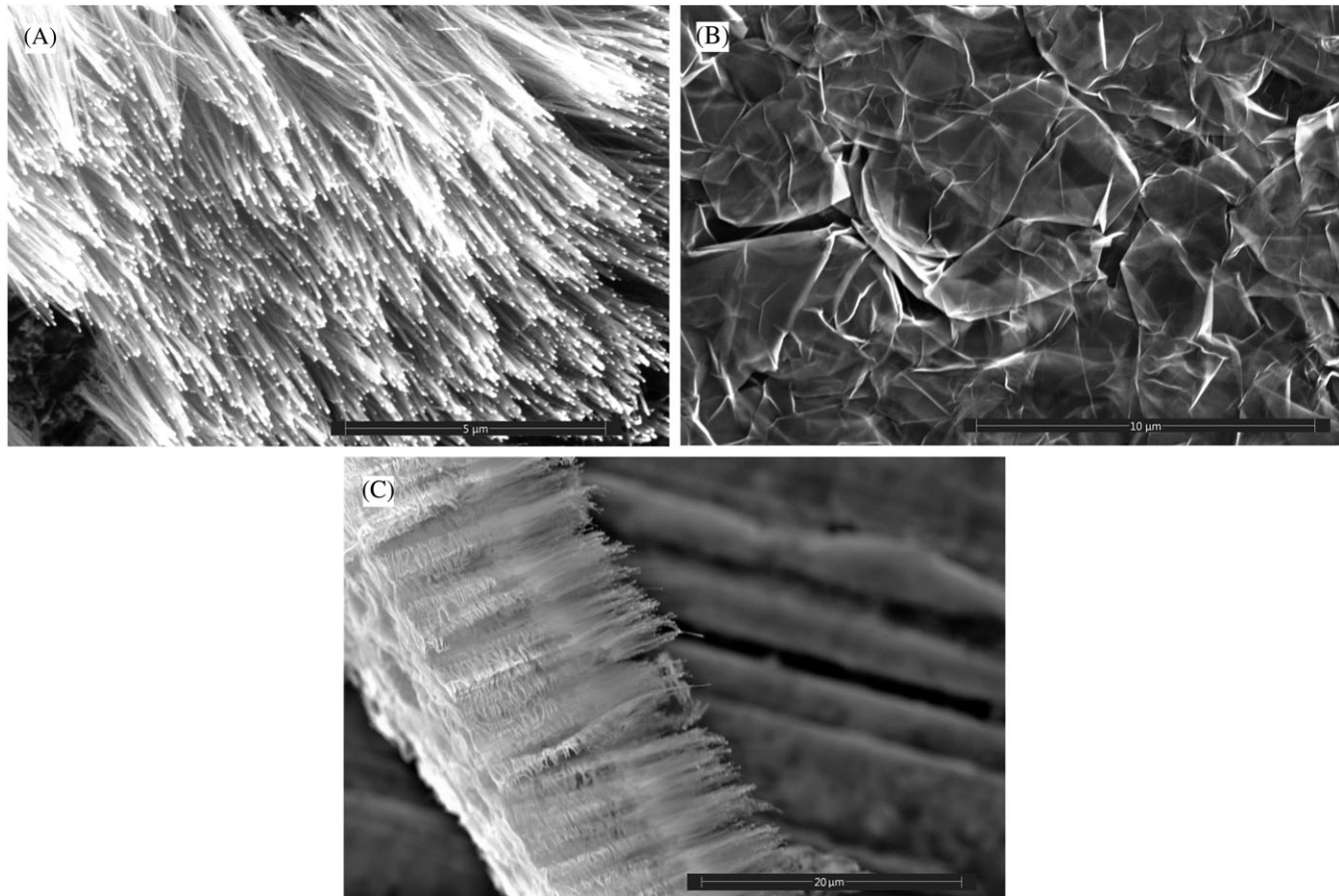


**FIGURE 3** SEM images of: A, VACNFs; B, pristine 3DG; C, N doped VACNF-3DG hybrid cross section

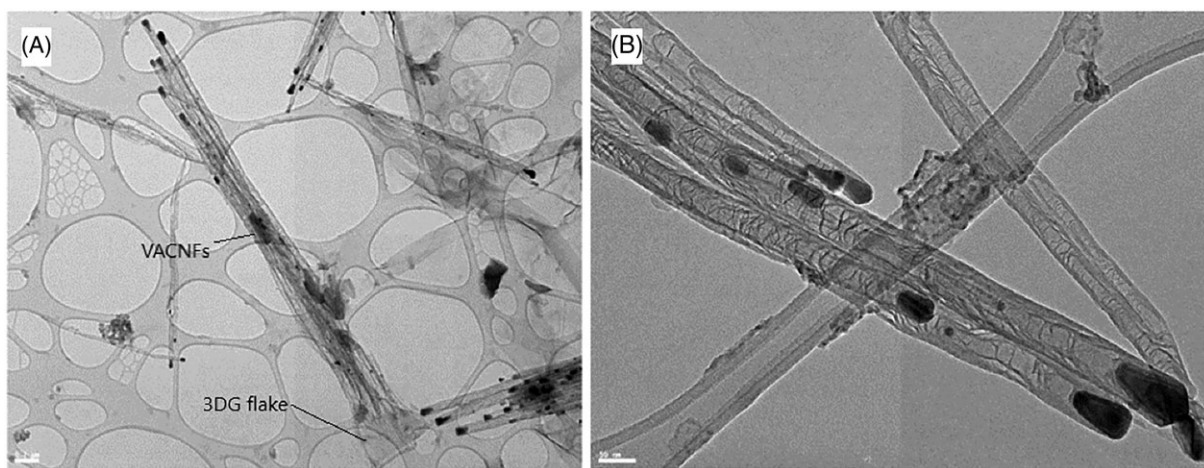


**FIGURE 4** TEM images with different magnification: A, VACNF-3DG—scale bar 0.2  $\mu$ m; B, VACNFs—scale bar 50 nm

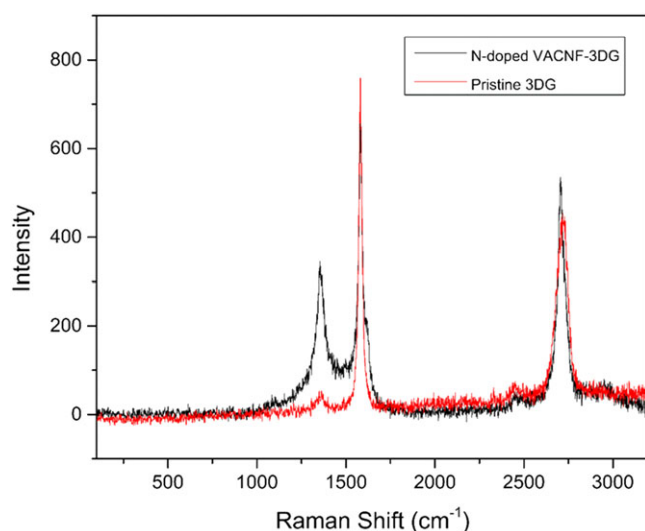


**FIGURE 5** RAMAN spectra for N-doped hybrid and pristine 3DG material

1580  $\text{cm}^{-1}$  was seen in the spectrum along with the overtone 2D around 2700  $\text{cm}^{-1}$ . The deposition of CNFs on 3DG led to an increase in D peak intensity around 1350  $\text{cm}^{-1}$  which represents disorder in the previous graphene structure. Another reason for high D peak could be attributed to the fact that the deposition of VACNF was done using PECVD, which generally creates a lot of radicals that affect the quality of carbon structure produced.<sup>36</sup> The first-order G band around 1580  $\text{cm}^{-1}$ , which is indicative of planar  $\text{sp}^2$  vibrations, was seen after deposition of VACNF as well. The RAMAN spectrum for the back side of the N-doped hybrid material was also taken, which looked like pristine 3DG (Figure S4). This indicates that the resultant material has a hybrid structure with one side as VACNF and another side as 3DG.

Carbon-based nanomaterials like graphene and CNTs are known to absorb methylene blue (MB) because of their high surface area. This can be used to qualitatively compare the surface areas of the carbon nanomaterials by analyzing the change in absorbance intensity during the UV-VIS spectroscopy.<sup>37,38</sup> UV-VIS spectral analysis was done on

25.4-mm square samples of pristine 3DG and N-doped VACNF-3DG to ascertain if the hybrid material had a greater surface area than the 3DG. Both the samples were soaked in 3 mL of a 5 mg/L MB aqueous solution for 20 hours in the dark followed by the UV-VIS measurements. From the UV-VIS spectrum in Figure 6, we observed a decrease in the MB intensity (peaks located at 665 nm) for the N-doped VACNF-3DG sample compared with pristine 3DG. This indicates more MB dye molecules were absorbed by the newly synthesized hybrid material confirming the improved ion accessible surface area after PECVD deposition of VACNF on 3DG.

The pristine 3DG measured 119.5° which dropped to 35.0° after VACNF deposition using PECVD shown in Figure 7. This contact angle was obtained a day after deposition. An attempt was made to measure contact angle an hour after deposition, but the surface was quite hydrophilic, so angle could not be well defined (Figure S5). Plasma treatment of graphene has been reported to improve the hydrophilicity of the material.<sup>39</sup> The pristine 3DG was found to be hydrophobic, and after VACNF deposition the N-doped hybrid material became hydrophilic.

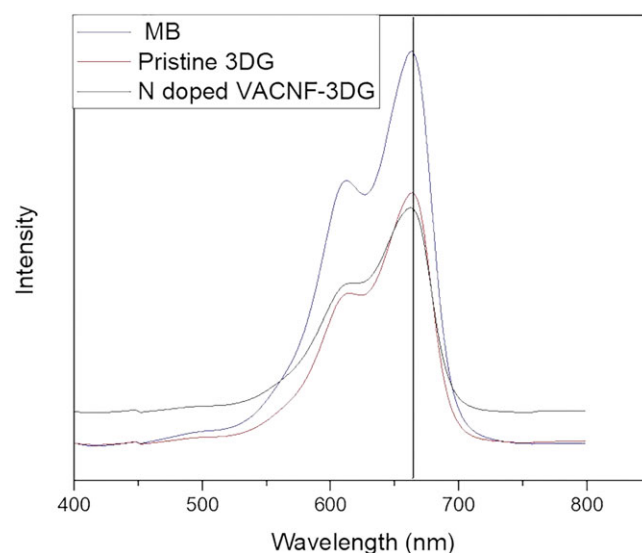


**FIGURE 6** UV-VIS absorption spectrum for N-doped hybrid, pristine 3DG, and MB at 665 nm

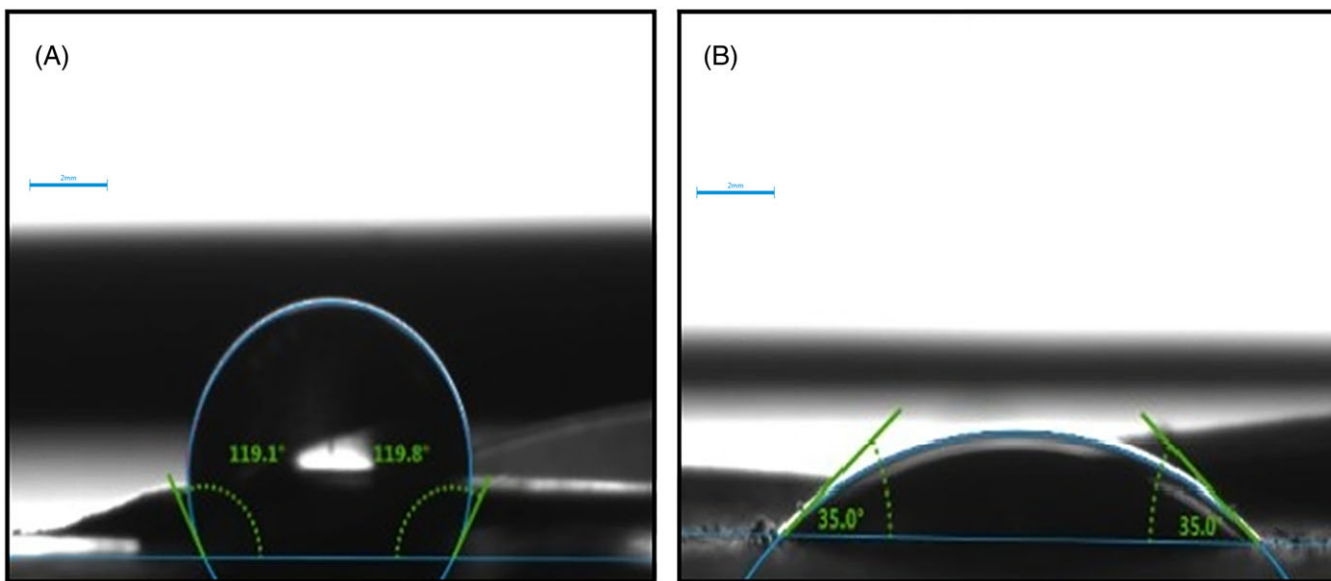


**FIGURE 7** Water contact angle: A, pristine 3DG; B, N doped VACNF-3DG hybrid material

Hydrophilicity of electrode material is beneficial for electrochemical device fabrication as it helps to improve the contact of the electrolyte with the electrode, thus enhancing the electron transport.

N doping was indicated by 5.4% nitrogen incorporation in the hybrid structure (Figure 8) as confirmed by XPS analysis. The deconvolution of N1s showed primarily four types of N based functional groups—pyridinic (398.4 eV), pyrrolic (399 eV), graphitic nitrogen (401.3 eV), and oxidized N (403 eV). The formation of pyridinic and graphitic N-type functional groups has been reported to improve the supercapacitance and electrocatalytic properties of CNT/graphene.<sup>40-42</sup> N doped graphene has also been demonstrated to function as an effective electrode for direct electron transfer in case of enzymatic biosensors.<sup>27</sup> In-situ N doping during deposition of CNT using ammonia has been reported previously by Misra et al.<sup>43</sup> In this study, in-situ N doping during PECVD of VACNFs was used. When VACNFs are deposited using hydrogen instead of ammonia, the resulting VACNFs exhibit p-type majority charge carriers due to excess oxygen impurities.<sup>44</sup> The addition of N via plasma doping can change the p-type carbon material to n-type, which can be used to obtain negative

Seebeck coefficients from carbon-based materials.<sup>45</sup> Thus, it can be concluded that N doped carbon structures offer appreciable advantages over their non-doped counterparts.

The electrochemical response of the hybrid material was compared with pristine 3DG using cyclic voltammetry. Different scan rates (25, 50, 125, 150, 250, 500 mV/s) were tested, and it was found that N doped hybrid material exhibited much higher current density in comparison to pristine 3DG (Figure 9). Nyquist plot for N doped hybrid material is shown in Figure S6. Here, two factors contributed towards the higher current density—N doping (Figure S7) and addition of VACNF to 3DG. The N doped hybrid exhibits a higher surface area which also leads to increased penetration of the electrolyte in the hybrid structure, thus resulting in a superior electrochemical response. The conductivity measurements were also made for N doped hybrid material, and it was found that the conductivity increased to 964 S/cm after plasma enhanced deposition process. This is well in agreement with the electrochemical data. Finally, it can be stated that the synthesized novel N doped hybrid material is a better choice for electrodes than pristine 3DG for different electrochemical applications like sensors, supercapacitors, and batteries.

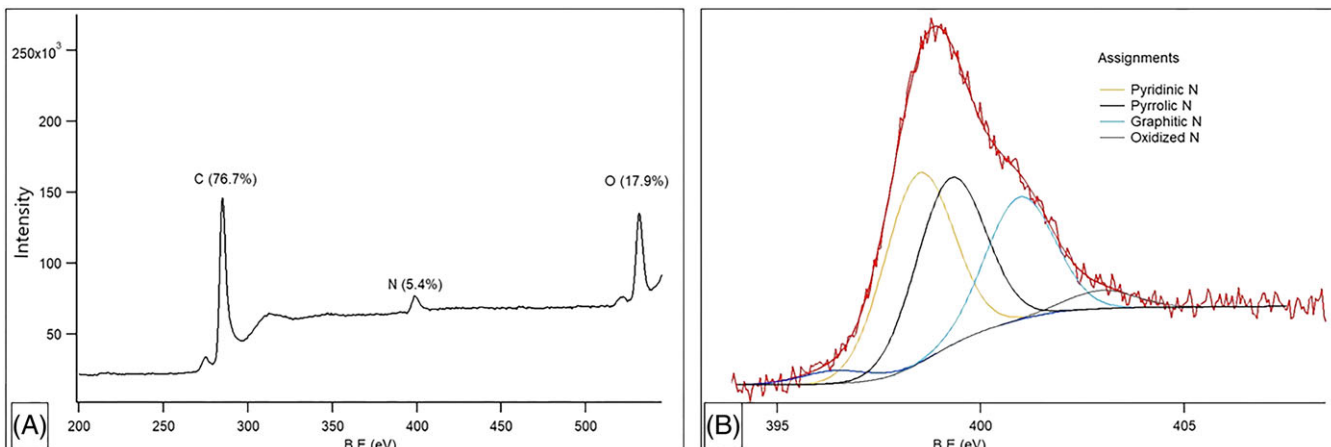


**FIGURE 8** XPS spectrum for N doped VACNF-3DG hybrid: A, overall survey; B, N1s deconvolution spectra

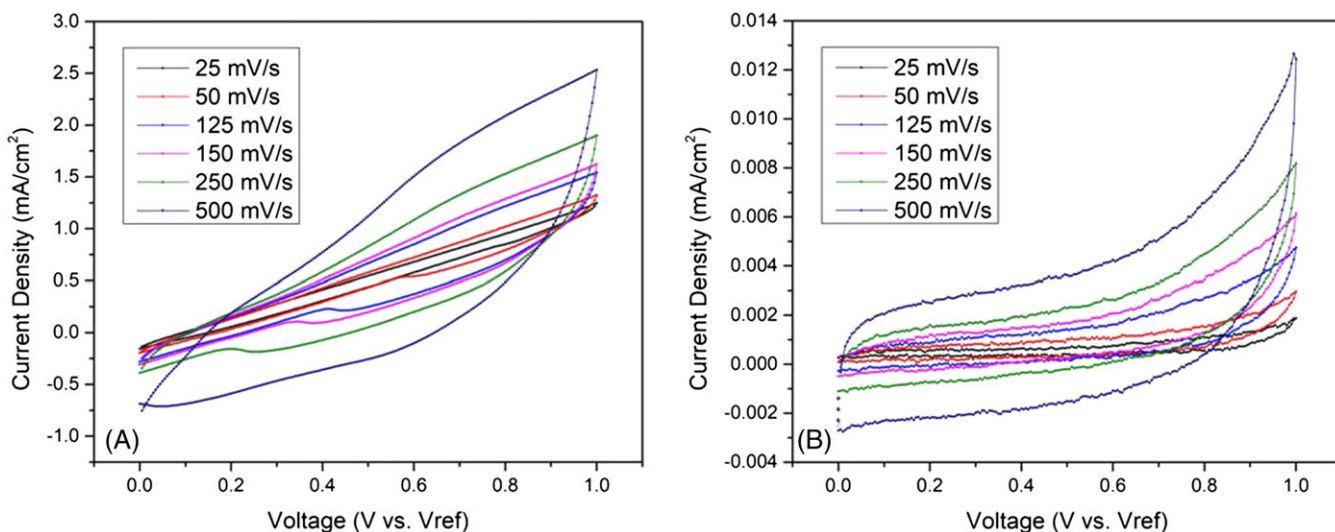


**FIGURE 9** CV curve: A, N doped VACNF-3DG hybrid; B, pristine 3DG at different scan rates

## 4 | CONCLUSION

A lightweight, N doped, three-dimensional VACNF-graphene hybrid structure was fabricated using a combination of thermal CVD and PECVD. The N doping of the hybrid material was proved by XPS. The OES was used to analyze the N-based species during PECVD, which went into the hybrid material to make it N doped. The increase in the surface area of 3DG after the deposition of VACNF material was evaluated qualitatively by UV-VIS spectroscopy. The current density for the hybrid material was much higher than compressed, pristine 3DG, which speaks for its potential of being used as electrodes for highly efficient energy storage devices and sensors. The free-standing nature of the material and the possibility of its scale-up make it more convenient for device fabrication. Further studies may include coating the hybrid structure with pseudocapacitive materials like polyaniline and manganese dioxide to further enhance the electrochemical response and fabricating energy storage devices using the N doped hybrid material as electrodes.

## ACKNOWLEDGEMENT

This work was partly supported by an NSF grant 1706489. We would also like to acknowledge the help from Mr Ron Flenniken at the UC Clean Room related to e-beam evaporation of the catalyst.

## ORCID

Siddharth Mishra  <https://orcid.org/0000-0002-4028-0671>

## REFERENCES

1. Melechko AV, Merkulov VI, McKnight TE, et al. Vertically aligned carbon nanofibers and related structures: controlled synthesis and directed assembly. *J Appl Phys.* 2005;97(4):041301. <https://doi.org/10.1063/1.1857591>
2. Meyyappan M, Delzeit L, Cassell A, Hash D. Carbon nanotube growth by PECVD: A review. *Plasma Sources Sci Technol.* 2003;12(2):205-216. <https://doi.org/10.1088/0963-0252/12/2/312>
3. Chen J, Bo Z, Lu G. Vertically-oriented graphene: PECVD synthesis and applications; 2015. <https://doi.org/10.1007/978-3-319-15302-5>
4. Vizireanu S, Stoica SD, Luculescu C, Nistor LC, Mitu B, Dinescu G. Plasma techniques for nanostructured carbon materials synthesis. A case study: carbon nanowall growth by low pressure expanding RF plasma. *Plasma Sources Sci Technol.* 2010;19(3). <https://doi.org/10.1088/0963-0252/19/3/034016>
5. Mesbahi A, Silva F. Study of the influence of gas flow on PECVD diamond growth: influence of the separate injection of gases. *J Phys D Appl Phys.* 2017;50(47):475203. <https://doi.org/10.1088/1361-6463/aa9167>
6. Boyd DA, Lin WH, Hsu CC, et al. Single-step deposition of high-mobility graphene at reduced temperatures. *Nat Commun.* 2015;6. [https://doi.org/10.1038/ncomms7620\(1\)](https://doi.org/10.1038/ncomms7620(1)).
7. Lone MY, Kumar A, Husain S, Zulfequar M, Husain M. Growth of carbon nanotubes by PECVD and its applications: a review. *Curr Nanosci.* 2017;13(5). <https://doi.org/10.2174/157341371366170317150807>
8. Ryu JH, Kim WS, Lee SH, Eom YJ, Park HK, Park KC. Vertically aligned carbon nanotube emitter on metal foil for medical X-ray imaging. *J Nanosci Nanotechnol.* 2013;13(10):7100-7103. <https://doi.org/10.1166/jnn.2013.7866>
9. Cantalini C, Valentini L, Armentano I, Lozzi L, Kenny JM, Santucci S. Sensitivity to NO<sub>2</sub> and cross-sensitivity analysis to NH<sub>3</sub>, ethanol and humidity of carbon nanotubes thin film prepared by PECVD. *Sens Actuators B.* 2003;95(1-3):195-202. [https://doi.org/10.1016/S0925-4005\(03\)00418-0](https://doi.org/10.1016/S0925-4005(03)00418-0)
10. Chang WS. Synthesis of free-standing carbon nanotube electrodes using plasma-enhanced chemical vapor deposition. In: 2016 IEEE International Conference on Plasma Science (ICOPS). IEEE; 2016:1-1. <https://doi.org/10.1109/PLASMA.2016.7534212>.
11. Mao S, Yu K, Chang J, Steeber DA, Ocola LE, Chen J. Direct growth of vertically-oriented graphene for field-effect transistor biosensor. *Sci Rep.* 2013;3. [https://doi.org/10.1038/srep01696\(1\)](https://doi.org/10.1038/srep01696(1)).
12. Choi JW, Youn SK, Park HG. Carbon micronymphaea: graphene on vertically aligned carbon nanotubes. *J Nanomater.* 2013;2013. (Cvd). <https://doi.org/10.1155/2013/734686>
13. Zhang M, Alvarez NT, Zhao D, et al. A corrugated graphene-carbon nanotube composite as electrode material. *Nano Life.* 2014;04(04):1441019. <https://doi.org/10.1142/S1793984414410190>
14. Zhao JG, Xing BY, Yang H, Pan QL, Li ZP, Liu ZJ. Growth of carbon nanotubes on graphene by chemical vapor deposition. *Xinxing Tan Cailiao/New Carbon Mater.* 2016;31(1):31-36. [https://doi.org/10.1016/S1872-5805\(16\)60002-1](https://doi.org/10.1016/S1872-5805(16)60002-1)
15. Kim YS, Kumar K, Fisher FT, Yang EH. Out-of-plane growth of CNTs on graphene for supercapacitor applications. *Nanotechnology.*

- 2012;23(1):015301. <https://doi.org/10.1088/0957-4484/23/1/015301>
16. Wu S, Shi E, Yang Y, Xu W, Li X, Cao A. Direct fabrication of carbon nanotube-graphene hybrid films by a blown bubble method. *Nano Res.* 2015;8(5):1746-1754. <https://doi.org/10.1007/s12274-014-0679-5>
17. Xia K, Zhan H, Gu Y. Graphene and carbon nanotube hybrid structure: a review. *Procedia IUTAM*. 2017;21:94-101. <https://doi.org/10.1016/j.piutam.2017.03.042>
18. Cao X, Shi Y, Shi W, et al. Preparation of novel 3D graphene networks for supercapacitor applications. *Small*. 2011;7(22):3163-3168. <https://doi.org/10.1002/smll.201100990>
19. Zhang L, DeArmond D, Alvarez NT, et al. Beyond graphene foam, a new form of three-dimensional graphene for supercapacitor electrodes. *J Mater Chem a*. 2016;4(5):1876-1886. <https://doi.org/10.1039/C5TA10031C>
20. Zhang L, Alvarez NT, Zhang M, et al. Preparation and characterization of graphene paper for electromagnetic interference shielding. *Carbon N Y*. 2015;82(C):353-359. <https://doi.org/10.1016/j.carbon.2014.10.080>
21. Huczko A, Kurcz M, Dąbrowska A, et al. Synthesis of 3-D graphene via combustion synthesis of magnesium and calcium/magnesium oxalates. *ECS J Solid State Sci Technol*. 2017;6(6):M3090-M3096. <https://doi.org/10.1149/2.0151706jss>
22. Huang Y, Li C, Lin Z. EDTA-induced self-assembly of 3D graphene and its superior adsorption ability for paraquat using a teabag. *ACS Appl Mater Interfaces*. 2014;6(22):19766-19773. <https://doi.org/10.1021/am504922v>
23. He J, Chen Y, Lv W, et al. Three-dimensional hierarchical graphene-CNT@Se: a highly efficient freestanding cathode for Li-Se batteries. *ACS Energy Lett.* 2016;1(1):16-20. <https://doi.org/10.1021/acsenergylett.6b00015>
24. Zhang W, Han C, Jia B, et al. A 3D graphene-based biosensor as an early microcystin-LR screening tool in sources of drinking water supply. *Electrochim Acta*. 2017;236:319-327. <https://doi.org/10.1016/j.electacta.2017.03.161>
25. Inagaki M, Toyoda M, Soneda Y, Morishita T. Nitrogen-doped carbon materials. *Carbon N Y*. 2018;132:104-140. <https://doi.org/10.1016/j.carbon.2018.02.024>
26. Faisal SN, Haque E, Noorbehesht N, et al. Pyridinic and graphitic nitrogen-rich graphene for high-performance supercapacitors and metal-free bifunctional electrocatalysts for ORR and OER. *RSC Adv.* 2017;7(29):17950-17958. <https://doi.org/10.1039/C7RA01355H>
27. Barsan MM, Prathish KP, Sun X, Brett CMA. Nitrogen doped graphene and its derivatives as sensors and efficient direct electron transfer platform for enzyme biosensors. *Sens Actuators B*. 2014;203:579-587. <https://doi.org/10.1016/j.snb.2014.07.019>
28. Lin YC, Teng PY, Yeh CH, Koshino M, Chiu PW, Suenaga K. Structural and chemical dynamics of pyridinic-nitrogen defects in graphene. *Nano Lett.* 2015;15(11):7408-7413. <https://doi.org/10.1021/acs.nanolett.5b02831>
29. Rybin M, Pereyaslavtsev A, Vasilieva T, et al. Efficient nitrogen doping of graphene by plasma treatment. *Carbon N Y*. 2016;96:196-202. <https://doi.org/10.1016/j.carbon.2015.09.056>
30. Jiang N, Wang HX, Zhang H, Sasaoka H, Nishimura K. Characterization and surface modification of carbon nanowalls. *J Mater Chem.* 2010;20(24):5070-5073. <https://doi.org/10.1039/c0jm00446d>
31. Desmaris V, Saleem MA, Shafiee S. Examining carbon nanofibers: properties, growth, and applications. *IEEE Nanotechnol Mag.* 2015;9(2):33-38. <https://doi.org/10.1109/MNANO.2015.2409394>
32. Zhang L, DeArmond D, Alvarez NT, et al. Flexible micro-supercapacitor based on graphene with 3D structure. *Small*. 2017;13(10):1603114. <https://doi.org/10.1002/smll.201603114>
33. Grulich O, Kregar Z, Modic M, et al. Treatment and stability of sodium hyaluronate films in low temperature inductively coupled ammonia plasma. *Plasma Chem Plasma Process*. 2012;32(5):1075-1091. <https://doi.org/10.1007/s11090-012-9387-7>
34. Suda Y, Okita A, Takayama J, et al. Carbon-nanotube growth in alcohol-vapor plasma. *IEEE Trans Plasma Sci*. 2009;37(7 SPEC. PART 1):1150-1155. <https://doi.org/10.1109/TPS.2009.2015451>
35. Dresselhaus MS, Dresselhaus G, Saito R, Jorio A. Raman spectroscopy of carbon nanotubes. *Phys Rep.* 2005;409(2):47-99. <https://doi.org/10.1016/j.physrep.2004.10.006>
36. Jia L, Sugiura H, Kondo H, et al. Effects of radical species on structural and electronic properties of amorphous carbon films deposited by radical-injection plasma-enhanced chemical vapor deposition. *Plasma Processes Polym.* 2016;13(7):730-736. <https://doi.org/10.1002/ppap.201500229>
37. Wang W, Liu W, Zeng Y, et al. A novel exfoliation strategy to significantly boost the energy storage capability of commercial carbon cloth. *Adv Mater.* 2015;27(23):3572-3578. <https://doi.org/10.1002/adma.201500707>
38. Wang G, Wang H, Lu X, et al. Solid-state supercapacitor based on activated carbon cloths exhibits excellent rate capability. *Adv Mater.* 2014;26(17):2676-2682. <https://doi.org/10.1002/adma.201304756>
39. Dey A, Chroneos A, Braithwaite NSJ, Gandhiraman RP, Krishnamurthy S. Plasma engineering of graphene. *Appl Phys Rev.* 2016;3(2). <https://doi.org/10.1063/1.4947188>
40. Zhang Y, Wang F, Zhu H, et al. Preparation of nitrogen-doped biomass-derived carbon nanofibers/graphene aerogel as a binder-free electrode for high performance supercapacitors. *Appl Surf Sci.* 2017;426:99-106. <https://doi.org/10.1016/j.apsusc.2017.07.127>
41. Li Y, Xu X, He Y, Jiang Y, Lin K. Nitrogen doped macroporous carbon as electrode materials for high capacity of supercapacitor. *Polymers (Basel)*. 2017;9(1):1-16. <https://doi.org/10.3390/polym9010002>
42. Kesavan T, Aswathy R, Raj IA, Kumar TP, Ragupathy P. Nitrogen-doped graphene as electrode material with enhanced energy density for next-generation supercapacitor application. *ECS J Solid State Sci Technol*. 2015;4(12):M88-M92. <https://doi.org/10.1149/2.0281512jss>
43. Misra A, Tyagi PK, Singh MK, Misra DS. FTIR studies of nitrogen doped carbon nanotubes. *Diamond Relat Mater.* 2006;15(2-3):385-388. <https://doi.org/10.1016/j.diamond.2005.08.013>
44. Vavro J, Llaguno MC, Fischer JE, et al. Thermoelectric power of [formula presented]-doped single-wall carbon nanotubes and the role of phonon drag. *Phys Rev Lett.* 2003;90(6):4. <https://doi.org/10.1103/PhysRevLett.90.065503>
45. Nonoguchi Y, Ohashi K, Kanazawa R, et al. Systematic conversion of single walled carbon nanotubes into n-type thermoelectric materials by molecular dopants. *Sci Rep.* 2013;3(1):3344. <https://doi.org/10.1038/srep03344>

## SUPPORTING INFORMATION

Additional supporting information may be found online in the Supporting Information section at the end of the article.

**How to cite this article:** Mishra S, Nguyen H, Adusei PK, Hsieh Y-Y, Shanov V. Plasma enhanced synthesis of N doped vertically aligned carbon nanofibers on 3D graphene. *Surf Interface Anal.* 2019;51:290-297. <https://doi.org/10.1002/sia.6604>